Sensors and Materials, Vol. 34, No. # (2022) 1–##
MYU Tokyo

S & M ####

Electrochemiluminescence Imaging Based on Bipolar Electrochemistry Using Commercially Available Anisotropic Conductive Films

Rise Akasaka,[1] Kosuke Ino,[2*] Tomoki Iwama,[1] Kumi Y. Inoue,[1,3] Yuji Nashimoto,[2,4] and Hitoshi Shiku[1,2**]

[1]Graduate School of Environmental Studies, Tohoku University, 6-6-11 Aramaki-aza Aoba, Aoba-ku, Sendai 980-8579, Japan
[2]Graduate School of Engineering, Tohoku University, 6-6-11 Aramaki-aza Aoba, Aoba-ku, Sendai 980-8579, Japan
[3]Center for Basic Education Faculty of Engineering, Graduate Faculty of Interdisciplinary Research, University of Yamanashi, 4-3-11, Takeda, Kofu 400-8511, Japan
[4]Frontier Research Institute for Interdisciplinary Sciences, Tohoku University, 6-3 Aramaki-aza Aoba, Aoba-ku, Sendai 980-8578, Japan

(Received November 24, 2021; accepted January 17, 2022: online published January 24, 2022)

Keywords: bipolar electrode, bipolar electrochemistry, electrochemiluminescence imaging, anisotropic conductive film

Electrochemical imaging with electrode arrays has been widely used to visualize chemicals and biomolecules. However, it is difficult to incorporate many sensors in a small area because of the large area of the leading connections and connector pads. To solve this problem, closed bipolar electrodes (BPEs) have been proposed as wireless electrochemical sensors, wherein many conductive materials are embedded in a thin film. However, it is laborious to prepare films with high-density BPEs. In this study, we demonstrate that commercially available anisotropic conductive films (ACFs) can be used as closed BPE films for electrochemiluminescence (ECL) imaging. Commercial ACFs are easily available without any fabrication equipment in a laboratory, which is a merit. The ACFs comprised conductive fibers embedded into a rubber film of 0.2 mm thickness. In the ACFs containing carbon fibers, the fiber diameter was 5–20 μm, and the fiber density was approximately 1×10^3 fibers/mm^2. As the films were made of rubber, they bend and stretch easily, and thus are useful for bending and stretching applications during assays. During ECL imaging, redox compounds react at the cathodic poles of BPEs, and ECL chemicals are oxidized at the opposite poles. In this study, we characterized ACFs for ECL imaging. Additionally, we presented a novel configuration of electrodes for ECL imaging based on a BPE array film, where it is unnecessary to insert an electrode into the ECL chemical solution. Finally, a moving droplet was electrochemically visualized to study the crosstalk between BPEs. To the best of our knowledge, this is the first report concerning ECL imaging based on BPEs using commercially available ACFs. In the future, this strategy will be coupled with biosensing for cell analyses and immunoassays.

*Corresponding author: e-mail: kosuke.ino@tohoku.ac.jp
**Corresponding author: e-mail: hitoshi.shiku.c3@tohoku.ac.jp
https://doi.org/10.18494/SAM3745

1. Introduction

Electrochemical imaging has been a widely used tool for analyzing biomolecules and chemicals. Moreover, several devices and systems have been proposed for electrochemical imaging. Electrochemical scanning probe microscopy,[1] such as scanning electrochemical microscopy,[2] scanning ion conductance microscopy,[3] and scanning electrochemical cell microscopy,[4] has been developed, wherein the samples are scanned using an electrode/capillary to visualize electrochemical reactions at the micro/nanometer level. However, the system might be unsuitable for rapidly imaging large areas and high-throughput analysis, owing to the long scan time. To overcome this challenge, electrode array devices have been proposed. CMOS techniques, which can provide highly sensitive assays, have been employed to incorporate many electrochemical/electric sensors into a small chip device.[5–10] However, it is still laborious to prepare many electrode sensors because of the large areas of electrodes containing sensor points, leading connections, and connector pads. To overcome these challenges, bipolar electrodes (BPEs) have been proposed, which act as electrochemical sensors without leading connections and connector pads.

Bipolar electrochemistry[11] has attracted much attention because of its advantages in analytical tools,[12] electrosynthesis,[13] and biofabrications.[14] A BPE is a conducting material in a solution with electrolytes, with a pair of driving electrodes placed in the solution. On applying a sufficient potential between the driving electrodes, anodic and cathodic reactions occur at both ends of the BPE, even in the absence of a direct Ohmic contact. By converting redox reactions at a cathodic (or anodic) pole to optical signals, such as electrochemiluminescence (ECL), at the other pole, BPEs can be used as wireless individual electrochemical sensors. For example, 1×10^3 individual BPEs (without leading connections and connector pads) can be operated using only a pair of driving electrodes,[15] which ultimately solves the aforementioned challenges. BPEs are roughly categorized into "open" and "closed" BPEs. In the case of open BPEs, conductors are placed in a single solution containing an electrolyte, and a pair of driving electrodes is inserted into the solution and connected to an external power supply. In the case of closed BPEs, the anodic and cathodic poles of the BPEs are physically separated and set in different solutions. As the reporter and sample cells are physically separated, crosstalk between them is prevented.

Several types of closed BPE device, including the probe type,[16–19] have been reported. Moreover, chip-based BPE arrays have been reported to detect biomarkers[20] and cellular functions, such as respiratory activity.[21] Recently, BPEs have been vertically embedded into thin films, resulting in the densification of electrochemical sensors.[22–29] One of the films was fabricated by patterning and pyrolyzing SU-8 films.[27] In the 15-μm-thick Parylene C, 1.5×10^5 carbon electrodes were embedded. In another approach, gold wires coated with epoxy resins were bundled and cut to prepare 4-mm-thick membranes.[23] Moreover, a BPE-array membrane was fabricated by depositing gold into the pores of a track-etched membrane using electroless plating.[22] However, it is still laborious to prepare these films. Hence, there is a need for an alternative film made of commercially available products. In this study, we focused on anisotropic conductive films (ACFs).

An ACF comprises a thermosetting resin and conductive particles in a film,[30] and has been widely used for anisotropic electrical conduction and adhesion. For example, ACFs are applied to connect several devices and printed circuit boards, and to inspect electrical parts and semiconductor devices in electronic components, semiconductors, information devices, and automobiles. Conductive fibers have also been used instead of particles for ACFs.[31] Herein, the configuration of the electrode is the same as that of BPE films in ECL imaging. Therefore, we assume that commercially available ACFs can be used as BPE films for ECL imaging. In this study, commercially available ACFs were characterized for this purpose. Moreover, a novel configuration of electrodes is presented for ECL imaging without the insertion of a driving electrode in an ECL solution. This configuration will be useful in microfluidic devices because the effect of solution resistance on the devices can be eliminated. This strategy will be used for bioimaging, including immunoassays and cell analyses in the future.

2. Materials and Methods

2.1 Commercially available ACFs as closed BPE arrays

Two types of commercially available ACF (Shin-Etsu Polymer, Japan) were used as closed BPEs. An outline of the ACFs is presented in Fig. 1. The ACFs comprised an insulated silicone rubber (thickness: 0.2 mm), and metal or carbon fibers were randomly arranged and vertically embedded into the rubber film.

2.2 General outline of ECL imaging based on bipolar electrochemistry

The ECL imaging scheme is shown in Fig. 2. An ECL solution, containing $[Ru(bpy)_3]^{2+}$ and tri-*n*-propylamine (TPA) as a co-reactant, was introduced on the side of the anodic poles of the BPEs in the ACF. Although several detailed processes for the ECL reaction have been discussed,[32] only one of the mechanisms is shown here. Briefly, $[Ru(bpy)_3]^{2+}$ is oxidized to $[Ru(bpy)_3]^{3+}$. TPA is also oxidized, resulting in the generation of a strongly reducing species. These two species then react to generate the excited state luminophore. In contrast, a $[Fe(CN)_6]^{3-}$ solution was introduced on the opposite side. These solutions were separated using the ACF. A

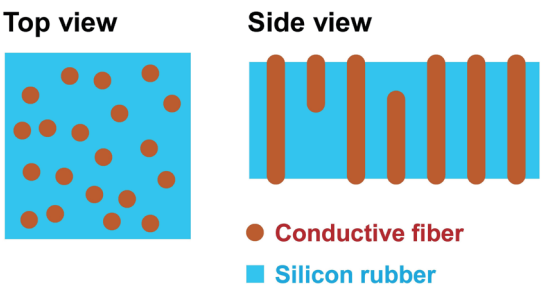

Fig. 1. (Color online) Illustration of ACFs with conductive fibers.

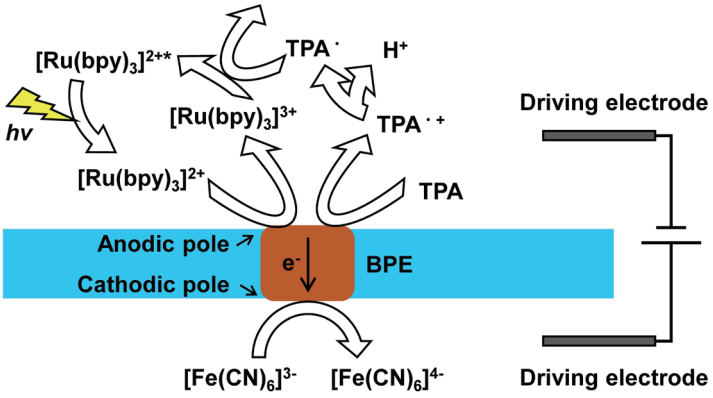

Fig. 2. (Color online) Scheme of ECL reactions using BPE. For simplicity, only a single BPE is illustrated. Although a single power supply is illustrated, a potentiostat was, in fact, used.

pair of driving electrodes was set in these solutions, and a suitable potential was applied to induce electrochemical reactions; this resulted in an ECL emission at the anodic poles of the BPEs. For setting electrochemical reactions at the BPEs to be rate-determining reactions, the size of the driving electrodes was sufficiently large.

2.3 ECL imaging and cyclic voltammetry using ACFs

ACFs with metal or carbon fibers were used in this study. Dulbecco's phosphate-buffered saline (D-PBS (−), Nacalai Tesque, Japan), containing 1 mM $[Fe(CN)_6]^{3-}$ (FUJIFILM Wako Pure Chemical Co., Japan), and PBS, containing 10 mM $[Ru(bpy)_3]^{2+}$ (Tokyo Chemical Industry Co., Ltd., Japan) and 100 mM TPA (FUJIFILM Wako Pure Chemical Co.), were used. In this study, a 100 mM solution was prepared by adding TPA to PBS. However, the TPA did not completely dissolve; therefore, the 100 mM TPA solution was vortexed well prior to each experiment. The PBS consists of 200 mg/L KCl, 200 mg/L KH_2PO_4, 8 g/L NaCl, and 1150 mg/L Na_2HPO_4, and its pH is approximately 7.4. Pt electrodes were used as the working and counter electrodes (WE and CE), and inserted into the ECL and $[Fe(CN)_6]^{3-}$ solutions, respectively. A Ag/AgCl reference electrode (sat. KCl) was inserted into the $[Fe(CN)_6]^{3-}$ solution. These electrodes were connected to a potentiostat (CompactStat, Ivium, The Netherlands). The ACFs were observed under a microscope (Eclipse Ti2, Nikon, Japan) with an EM-CCD camera (ImagEM X2, Hamamatsu Photonics K.K., Japan). The potential was scanned from 0 to −1.5 V at 50 mV/s, and the ECL signals were obtained with a 100 ms exposure time from the top in a dark room.

2.4 ECL imaging based on the configuration of three separated solutions

As a demonstration of the novel configuration of electrodes for ECL imaging based on the BPE film, the ACF was floated in the PBS containing 25 mM $[Ru(bpy)_3]^{2+}$ and 100 mM TPA,

and two glass micropipettes (calibrated micropipette, 10 μL) filled with a solution containing 100 mM $[Fe(CN)_6]^{3-}$, 100 mM $[Fe(CN)_6]^{4-}$, and 100 mM KCl were set on the ACF. The inner diameter at the tip was controlled to be 175−500 μm by heating and pulling. A meniscus of the $[Fe(CN)_6]^{3-/4-}$ solution at the tip formed on the ACF. Ag/AgCl wires were inserted into the micropipettes and connected to a potentiostat (1010mM8, Hokuto Denko, Japan). A potential of 3.0 or −3.0 V was applied to induce an ECL emission. The ECL signals were monitored from the bottom under a microscope (IX71, Olympus, Japan) and a CCD camera (DP71, Olympus) with an exposure time of 30 s in a dark room. A schematic illustration is shown in Sect. 3.3.

2.5 ECL imaging of a moving droplet using ACFs

A moving droplet was visualized using ACFs with carbon fibers. The ACFs were floated in the PBS containing 25 mM $[Ru(bpy)_3]^{2+}$ and 100 mM TPA. Two Ag/AgCl wires were inserted into the ECL solution as the CE and reference electrode (RE). A glass micropipette containing a solution with 100 mM $[Fe(CN)_6]^{3-}$ and 100 mM $[Fe(CN)_6]^{4-}$, and 100 mM KCl was set on the ACFs, and a Ag/AgCl wire was inserted into the solution. A potential of 1.5 V was applied to induce ECL, and the micropipette was moved at 10 μm/s using an XYZ stage (Stepping Motor, Suruga Seiki, Japan). ECL signals were obtained from the bottom, with a 3 s exposure time. A schematic illustration is shown in Sect. 3.4.

3. Results and Discussion

3.1 Commercially available ACFs as closed BPE arrays

Figure 3 shows photographs of the ACFs. There were no cracks and holes in the films, indicating that the ACFs can be used as closed BPEs. Owing to the transparency of the ACFs, the letters comprising “TOHOKU UNIVERSITY” were readable behind the ACFs [Fig. 3(A)], and its features find use in bioanalysis such as assays in cell culture. Moreover, the ACFs were easily stretched to over 150% [Fig. 3(B)] and bent [Fig. 3(C)], and did not crack [Figs. 3(D) and 3(E)]. Therefore, the rubber films are superior to previous BPE films in stretching and bending applications, such as wearable sensing devices[33] and the electrochemical imaging of cells applied with mechanical stress.[34]

Unfortunately, the size and shape were non-uniform, and the sizes of the carbon and metal fibers were 5–20 and 20–100 μm, respectively. Furthermore, the fibers were not arranged precisely in the arrays. The densities of the carbon and metal fibers were approximately 1×10^3 and 1×10^2 fibers/mm^2, respectively. For imaging, sensors should have the same performance and should be precisely arranged in an array. Therefore, the ACFs are inferior to previous BPE films[22–27] for ECL imaging based on BPEs. In contrast, commercial ACFs are easily available without any fabrication equipment and have an extensive lineup; hence, they are attractive compared with previous BPE films.

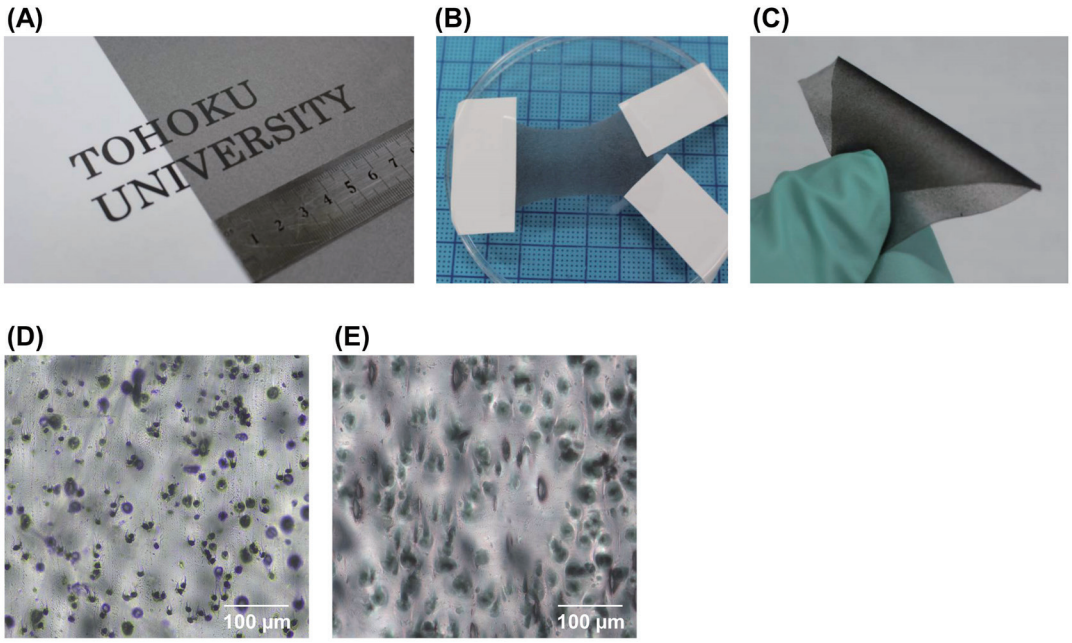

Fig. 3. (Color online) Photographs of ACFs with carbon fibers. (A) Transparency of ACFs. (B) Stretched and (C) bent ACFs. (D, E) Microphotographs. (E) Stretched ACFs.

3.2 ECL imaging and cyclic voltammetry using ACFs

Figure 4(A) shows a schematic of ECL imaging using the ACFs. When using the ACFs with metal fibers, a potential of −0.5 V was insufficient to induce ECL at the anodic poles. As the negative potential increased, the ECL signals gradually increased; however, ECL emissions were obtained from less than 20% BPEs at −1.5 V [Fig. 4(B)]. Although a red emission was observed, ECL images were black and white because the levels of photons detected by the EM-CCD camera are displayed in gray scale. Additionally, the carbon fibers were successfully applied to ECL imaging [Fig. 4(C)]. The rate of the BPEs for the ECL emission was above 35% at −1.5 V and higher while using the metal fibers. The low rate was due to the lack of fiber penetration [Fig. 1(B)], an insufficient potential for the materials, and/or their heterogeneities. The number of working carbon fibers for the ECL emission was larger than that of metal fibers. These results indicate that the ACFs with carbon fibers are suitable for ECL imaging. Therefore, the ACFs with carbon fibers were characterized in the following experiments.

Figure 4(D) shows a cyclic voltammogram using the ACFs with carbon fibers. The cyclic voltammogram provided information on the redox reactions occurring on the BPEs, because the driving electrodes were sufficiently large for rate-determining reactions at the BPEs. The reduction current gradually increased from approximately −0.7 V, and the potential corresponded to that for the ECL emission, indicating that the cyclic voltammogram might mainly originate from the electrochemical reaction of the luminophore, $[Ru(bpy)_3]^{2+}$, at the anodic poles of the BPEs. Thus, the cyclic voltammogram also supported the ECL images. In a previous study,

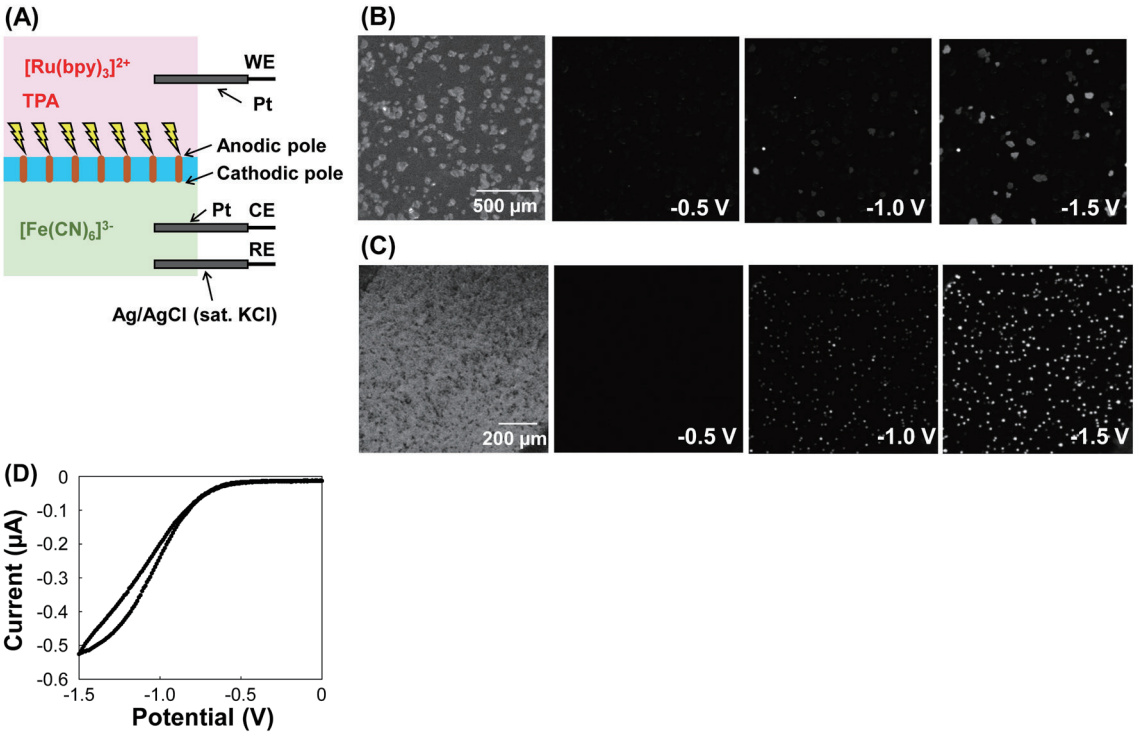

Fig. 4. (Color online) ECL imaging based on bipolar electrochemistry using ACFs. (A) Schematic. Bright field and ECL images using ACFs with (B) metal and (C) carbon fibers. (D) Cyclic voltammogram using ACF with carbon fibers. Film area: 1.6 mm^2. Scan rate: 50 mV/s.

pyrolyzed carbon BPEs and 2-(dibutyl)aminoethanol, instead of TPA, were used, and ECL responses were obtained from approximately 1.1 V,[27] which was roughly similar to our results.

Under these experimental conditions, the concentration of $[Fe(CN)_6]^{3-}$ was lower than that of the ECL chemicals; we assumed that the current depended on the concentration of $[Fe(CN)_6]^{3-}$. When the radius of the cathodic poles of the BPEs, the number of reaction electrons at the reaction, the concentration of $[Fe(CN)_6]^{3-}$, its diffusion coefficient, and the number of cathodic poles are set to be 10 μm, 1, 1 mM, 7×10^{-10} m^2/s, and 560, respectively, the theoretical limiting current was calculated to be approximately 1.5 μA using an equation for a disk microelectrode,[35] which was three times the experimental value. The mismatch is due to the high density of the cathodic poles of the BPEs and the overlap of diffusion. These results indicate that the dissolved oxygen did not react on the cathodic poles of the BPEs when −1.5 V was applied.

3.3 ECL imaging based on the configuration of three separated solutions

In general, the driving electrodes were inserted into the reporter and sample solutions. However, for a semi-closed environment, such as that of microfluidic devices, it might be difficult to insert an electrode. Therefore, if the driving electrodes can be set on one side of a

BPE film, it would expand its application. Thus, a novel configuration was proposed, as shown in the scheme in Fig. 5(A), and ECL imaging was conducted using three separated solutions. The ECL signals were obtained only in the areas of the meniscus [Fig. 5(B)], indicating that the configuration was successful. The electrochemical reactions shown in Fig. 2 occurred at the cathodic and anodic poles of the BPEs where the WE was set. On the BPEs where the CE/RE was set, $[Fe(CN)_6]^{4-}$ was oxidized at the anodic poles and H_2 was generated at the cathodic poles. As the additional potential was required, 3.0 V was used instead of 1.5 V. On switching the potentials from 3.0 to −3.0 V, the ECL signals were obtained at the meniscus in another micropipette, which was reasonable. In this configuration, it is unnecessary to insert a driving electrode into an ECL solution, which is superior to the conventional configuration, as shown in Fig. 2.

3.4 ECL imaging of a moving droplet using BPE arrays

It is crucial to eliminate crosstalk at high spatial resolutions. To characterize the crosstalk between the BPEs, the droplet moved, and the ECL emission was monitored [Fig. 6(A)]. The ACFs had good water repellency, and the droplet did not spread excessively. The ECL emissions were successfully observed only in the areas of the meniscus, indicating that there was no crosstalk [Fig. 6(B)].

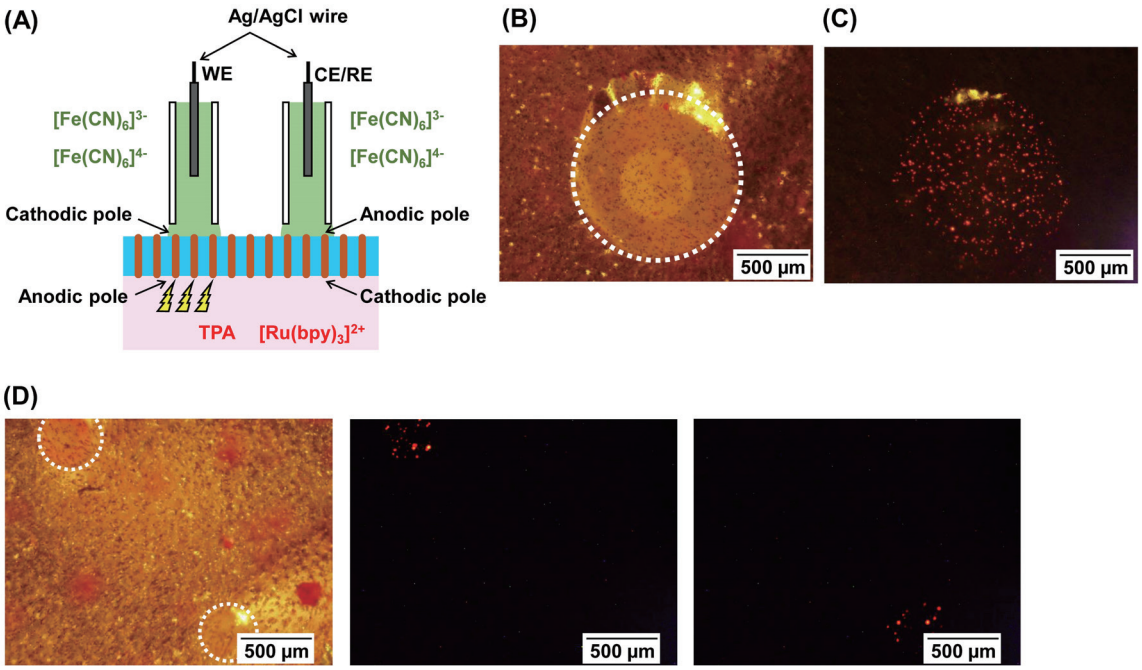

Fig. 5. (Color online) ECL imaging based on the configuration of three separated solutions using ACFs with carbon fibers. (A) Schematic when 3.0 V is applied. (B) Bright field and (C) ECL images of the meniscus at 3.0 V. (D) ECL images during the potential switch from 3.0 to −3.0 V. White dotted circles indicate the edge of the meniscus.

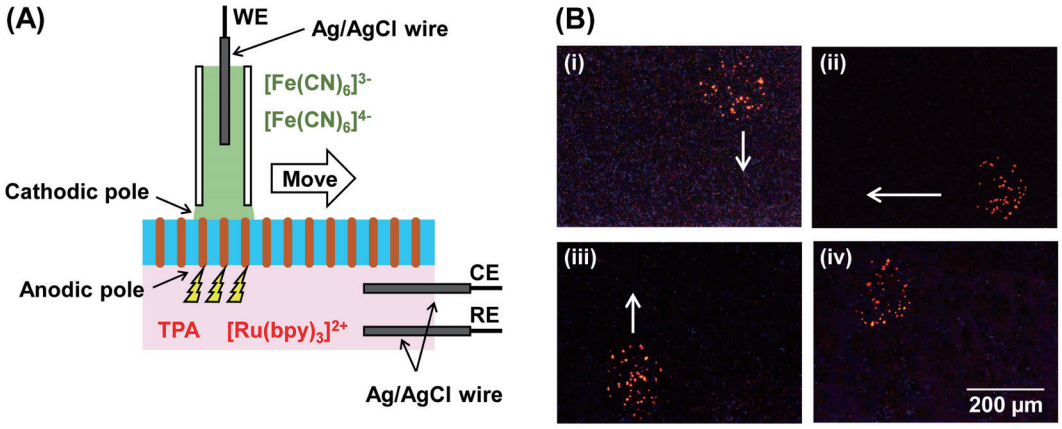

Fig. 6. (Color online) ECL imaging of moving droplet using ACFs with carbon fibers. (A) Schematic. (B) Time course of ECL images at 1.5 V. The contrast of the ECL images was modified to make them clear.

4. Conclusions

We successfully performed ECL imaging using commercially available ACFs. To the best of our knowledge, this is the first report on ECL imaging based on bipolar electrochemistry using commercially available ACFs. Two types of ACF were characterized, and carbon fibers were found suitable for ECL imaging. Although $[Fe(CN)_6]^{3-}$ was converted to ECL signals in this study, if biomolecules and enzymatic products can be converted to ECL signals, ACFs can be utilized for immunoassays and cell analyses. For example, if dissolved oxygen is converted to ECL signals,[21] the respiratory activity of tissues and organs can be evaluated using ECL images. In this study, closed BPEs were used wherein the sample and reporter chambers were physically separated and ECL chemicals do not affect samples in future applications, which makes the system superior to another ECL system wherein the biosamples were placed in an ECL solution.[36] In this study, we present a novel configuration for ECL imaging where electrodes were set on only one side. The configuration is useful when the insertion of electrodes into the sample or reporter solution is limited, such as in microfluidic devices.

Acknowledgments

This work was supported by Grants-in-Aid for Scientific Research (Nos. 20H00619, 18H01840, and 18H01999) and a Grant-in-Aid for Early-Career Scientists (No. 19K20658) from JSPS. This work was also supported by the Shimadzu Science Foundation, Electrochemical Society of Japan, Japan Association for Chemical Innovation, and JST COI (No. JPMJCE13).

References

1 A. Kumatani and T. Matsue: Curr. Opin. Electrochem. **22** (2020) 228. https://doi.org/10.1016/j.coelec.2020.07.010
2 Y. Zhou, Y. Takahashi, T. Fukuma, and T. Matsue: Curr. Opin. Electrochem. **29** (2021) 100739. https://doi.org/10.1016/j.coelec.2021.100739
3 E. Tognoni: Curr. Opin. Electrochem. **28** (2021) 100738. https://doi.org/10.1016/j.coelec.2021.100738

4 C. L. Bentley, M. Kang, and P. R. Unwin: Curr. Opin. Electrochem. **6** (2017) 23. https://doi.org/10.1016/j.coelec.2017.06.011
5 K. Ino, W. Saito, M. Koide, T. Umemura, H. Shiku, and T. Matsue: Lab Chip **11** (2011) 385. https://doi.org/10.1039/C0LC00437E
6 K. Y. Inoue, M. Matsudaira, R. Kubo, M. Nakano, S. Yoshida, S. Matsuzaki, A. Suda, R. Kunikata, T. Kimura, R. Tsurumi, S. Toshihito, I. Kosuke, S. Hitoshi, S. Shiro, E. Masayoshi, and M. Tomokazu: Lab Chip **12** (2012) 3481. https://doi.org/10.1039/C2LC40323D
7 Y. Kanno, K. Ino, H. Abe, C. Sakamoto, T. Onodera, K. Y. Inoue, A. Suda, R. Kunikata, M. Matsudaira, and H. Shiku: Anal. Chem. **89** (2017) 12778. https://doi.org/10.1021/acs.analchem.7b03042
8 K. Gamo, K. Nakazato, and K. Niitsu: IEICE Trans. Electron. E100.C (2017) 602. 10.1587/transele.E100.C.602
9 H. Doi, B. Parajuli, T. Horio, E. Shigetomi, Y. Shinozaki, T. Noda, K. Takahashi, T. Hattori, S. Koizumi, and K. Sawada: Sens. Actuators, B **335** (2021) 129686. https://doi.org/10.1016/j.snb.2021.129686
10 X. Yuan, M. Schröter, M. E. J. Obien, M. Fiscella, W. Gong, T. Kikuchi, A. Odawara, S. Noji, I. Suzuki, J. Takahashi, A. Hierlemann, and U. Frey: Nat. Commun. **11** (2020) 4854. 10.1038/s41467-020-18620-4
11 S. E. Fosdick, K. N. Knust, K. Scida, and R. M. Crooks: Angew. Chem. Int. Ed. **52** (2013) 10438. https://doi.org/10.1002/anie.201300947
12 S. M. binti Fakhruddin, K. Ino, K. Y. Inoue, Y. Nashimoto, and H. Shiku: Electroanalysis (in press). https://doi.org/10.1002/elan.202100153
13 N. Shida, Y. Q. Zhou, and S. Inagi: Accounts Chem. Res. **52** (2019) 2598. https://doi.org/10.1021/acs.accounts.9b00337
14 K. Ino, T. Matsumoto, N. Taira, T. Kumagai, Y. Nashimoto, and H. Shiku: Lab Chip **18** (2018) 2425. https://doi.org/10.1039/C8LC00465J
15 K.-F. Chow, F. Mavré, J. A. Crooks, B.-Y. Chang, and R. M. Crooks: J. Am. Chem. Soc. **131** (2009) 8364. https://doi.org/10.1021/ja902683f
16 T. Iwama, Y. Guo, S. Handa, K. Y. Inoue, T. Yoshinobu, F. Sorin, and H. Shiku: Adv. Mater. Technol. (2021) 2101066. https://doi.org/10.1002/admt.202101066
17 C. S. Santos, F. Conzuelo, V. Essmann, M. Bertotti, and W. Schuhmann: Anal. Chim. Acta **1087** (2019) 36. https://doi.org/10.1016/j.aca.2019.08.049
18 S. M. B. Fakhruddin, K. Y. Inoue, R. Tsuga, and T. Matsue: Electrochem. Commun. **93** (2018) 62. https://doi.org/10.1016/j.elecom.2018.06.006
19 J. P. Guerrette, S. M. Oja, and B. Zhang: Anal. Chem. **84** (2012) 1609. https://doi.org/10.1021/ac2028672
20 M.-S. Wu, Z. Liu, H.-W. Shi, H.-Y. Chen, and J.-J. Xu: Anal. Chem. **87** (2015) 530. https://doi.org/10.1021/ac502989f
21 K. Ino, R. Yaegaki, K. Hiramoto, Y. Nashimoto, and H. Shiku: ACS Sens. **5** (2020) 740. https://doi.org/10.1021/acssensors.9b02061
22 T. Iwama, K. Y. Inoue, H. Abe, T. Matsue, and H. Shiku: Analyst **145** (2020) 6895. https://doi.org/10.1039/D0AN00912A
23 T. Iwama, K. Y. Inoue, H. Abe, and T. Matsue: Chem. Lett. **47** (2018) 843. https://doi.org/10.1246/cl.180303
24 J. P. Guerrette, S. J. Percival, and B. Zhang: J. Am. Chem. Soc. **135** (2013) 855. https://doi.org/10.1021/ja310401b
25 S. M. Oja and B. Zhang: Anal. Chem. **86** (2014) 12299. https://doi.org/10.1021/ac5035715
26 T. J. Anderson, P. A. Defnet, R. A. Cheung, and B. Zhang: J. Electrochem. Soc. **168** (2021) 106502. https://doi.org/10.1149/1945-7111/ac2acc
27 T. J. Anderson, P. A. Defnet, and B. Zhang: Anal. Chem. **92** (2020) 6748. https://doi.org/10.1021/acs.analchem.0c00921
28 T. Iwama, M. Komatsu, K. Y. Inoue, and H. Shiku: ChemElectroChem **8** (2021) 3492. https://doi.org/10.1002/celc.202100675
29 H. Abe, T. Iwama, and Y. Guo: Electrochem **2** (2021) 472. https://doi.org/10.3390/electrochem2030031
30 S.-H. Lee and K.-W. Paik: J. Electron. Mater. **46** (2017) 167. https://doi.org/10.1007/s11664-016-4895-5
31 M. D. Diop, M. Radji, A. A. Hamoui, Y. Blaquiere, and R. Izquierdo: IEEE Trans. Compon. Pack. Manuf. Technol. **3** (2013) 581. https://doi.org/10.1109/tcpmt.2013.2243203
32 W. J. Miao, J. P. Choi, and A. J. Bard: J. Am. Chem. Soc. **124** (2002) 14478. https://doi.org/10.1021/ja027532v
33 Y. R. Yang and W. Gao: Chem. Soc. Rev. **48** (2019) 1465. https://doi.org/10.1039/c7cs00730b
34 Y. L. Liu, Z. H. Jin, Y. H. Liu, X. B. Hu, Y. Qin, J. Q. Xu, C. F. Fan, and W. H. Huang: Angew. Chem. Int. Ed. **55** (2016) 4537. https://doi.org/10.1002/anie.201601276
35 A. Minguzzi, M. A. Alpuche-Aviles, J. R. López, S. Rondinini, and A. J. Bard: Anal. Chem. **80** (2008) 4055. https://doi.org/10.1021/ac8001287
36 K. Hiramoto, K. Ino, K. Komatsu, Y. Nashimoto, and H. Shiku: Biosens. Bioelectron. **181** (2021) 113123. https://doi.org/10.1016/j.bios.2021.113123